Long-Wavelength Optical Phonons and Phase Transitions in SbSI†

D. K. Agrawal and C. H. Perry
Solid State Spectroscopy Laboratory, Department of Physics, Northeastern University, Boston, Massachusetts 02115
(Received 15 January 1971)

The polarized infrared and Raman spectra of SbSI have been measured in the paraelectric and the ferroelectric phases as a function of temperature. The frequencies and the symmetries of most of the optically active phonons have been determined in both phases. A strongly temperature-dependent A mode which is simultaneously Raman- and infrared-active has been observed in the ferroelectric phase. This low-frequency mode completely accounts for the temperature dependence of the dielectric constant along the ferroelectric axis. Kramers-Kronig analyses of the polarized infrared spectra yielded the dielectric response functions and the TO- and LO-phonon frequencies at the Γ point of the Brillouin zone. A very-low-frequency soft A_u mode (≈ 9 cm^{-1}) accounts for more than 90% of the static dielectric constant at room temperature. It has been found that both infrared and Raman data are consistent with the symmetry change from C_{2h}^2 (two formula units/unit cell) to C_2^2 (two formula units/unit cell) at 288 °K, which finally changes to C_2^2 (four formula units/unit cell) at 233 °K. An intensity maximum in the Raman spectrum at ~240 °K is due to resonant Raman effects where the energy band gap is approximately equal to the laser excitation source energy of 1.96 eV.

I. INTRODUCTION

Long-wavelength optical phonons of the ferroelectric semiconductor antimony sulphoiodide (SbSI) have been investigated using far-infrared and Raman spectroscopic techniques.[1–5] In the present work, both infrared and Raman studies have been carried out in the same crystals at several temperatures in the paraelectric and the ferroelectric phases. Both polarizations ($E \parallel c$ and $E \perp c$) and all Raman tensor components were obtained in the entire phonon region 20–400 cm^{-1}. The complete symmetry analysis of the Raman-active and infrared-active phonon frequencies according to the various irreducible representations of the proposed space groups of SbSI has been carried out in order to confirm the proposed space groups and understand the mechanism of the phase transitions. SbSI undergoes a first-order ferroelectric phase transition[6,7] at about 288 °K.[8] The full crystal-space-group symmetry changes from D_{2h}^{16} ($Pnam$) in the paraelectric phase to C_{2v}^9 ($Pna2_1$) in the ferroelectric phase. Both phases have four formula units per unit cell. Below T_c it has been shown that Sb and S atoms shift along the ferroelectric c axis with respect to iodine by 0.20 and 0.05 Å, respectively.[9] This indicates that the phase transition should be of a displacive type.[10] A second-order phase transition at about 233 °K has been reported recently and the space group finally changes to C_2^2 ($P2_1$) with four formula units per unit cell.[11] However, no anomaly in the dielectric constant was observed at this transition.[12] It is unlikely that any soft mode should characterize such a transition, but the symmetry changes should manifest themselves in the infrared and Raman spectra.

The evidence of the displacive character of the first-order phase transition has been obtained from the soft-mode behavior observed in Raman scattering.[2] In the ferroelectric phase the lowest-frequency mode (~50 cm^{-1} at 100 °K) accounted completely for the temperature dependence of the static dielectric constant in agreement with Cochran's theory of displacive ferroelectrics.[13] Recent Raman scattering experiments in the same temperature range[3] suggest that coupling occurs between the soft mode and another low-frequency mode (very weak mode at 100 °K) of the same symmetry resulting in level repulsion and intensity transfer of the two modes. Our Raman scattering measurements for the α_{zz} Raman tensor component tend to favor the existence of another weak band at ~30 cm^{-1} as observed by Harbeke *et al.*[3] However, our infrared measurements do not indicate the existence of such a band in either the paraelectric phase or the ferroelectric phase.

Recently Petzelt[1] measured the far-infrared reflectivity spectra of SbSI in the wave-number region 30–400 cm^{-1} using a Fourier-transform Michelson interferometer with a room-temperature Golay detector. In the present infrared data, the signal-to-noise ratio has been improved by at least an order of magnitude using a liquid-helium-cooled gallium-doped germanium bolometer detector. This detector was used in the frequency region 20–250 cm^{-1} where the energy of the conventional infrared sources is particularly low. In the frequency region 250–400 cm^{-1}, our data were also obtained with a Golay detector and are in agreement with Petzelt's measurements. However, in the low-frequency range for $c \perp E$, Petzelt reported

bands at 56 and 66 cm^{-1} which were not observed in our infrared data. For $c \| E$, our measurements are in reasonable agreement with those of Sugawara and Nakamura[5] and the low-frequency soft mode in the paraelectric phase is probably situated below 10 cm^{-1} and not as reported by Petzelt at ~22 cm^{-1}.

II. EXPERIMENTAL

The single crystals used in the Raman investigations were thin needles (about 1-mm^2 cross section), with the c axis along the needle axis. The crystals were grown from the vapor phase, and the growth faces were perpendicular to the [100] and [010] directions. No attempt was made to positively identify the crystal a and b axes as only relatively minor intensity changes were observed by interchanging the designated x and y directions.

The Raman spectra were recorded using an 80-mW Spectra-Physics model No. 125 He-Ne laser and Spex model No. 1400 double monochromator. The detector was an ITT FW-130 photomultiplier tube with S-20 photocathode and photoelectron counting detection electronics. An oblique angle-reflection geometry was used and the spectral resolution $\Delta\nu$ was normally ~2 cm^{-1}. The temperature control both above and below room temperature was achieved with a variable-temperature continuous-gas-transfer cryostat with fused quartz windows.[14] The temperature was monitored by a copper-constantan thermocouple mounted on the small bracket holding the crystal. The temperature stability of ±1 °K could thus be achieved.

Figure 1 shows the Raman scattering geometries for measuring the polarizability Raman tensor components. Only TO phonons were excited as the polarization of the incident beam was perpendicular to the scattering plane for observing all Raman-active phonon frequencies listed in Table II. The scattering geometry was approximately backward due to the high refractive index (~3–5) of these crystals.[15]

For the infrared measurements, a mosaic sample was prepared from several SbSI needles and mounted such that their c axes were parallel. The sample was about 5×10 mm^2 in area and had a unique c axis parallel to the longer side.

The reflectance spectra were measured with an R.I.I.C. FS-520 Fourier spectrometer (Michelson type) adapted for 12-bit analog-to-digital conversion.[16] A mercury-arc source in conjunction with a liquid-helium-cooled Ga-doped germanium bolometer was used from 20 to 200 cm^{-1}. A Nernst glower with a Golay pneumatic cell was used from 150–400 cm^{-1}. A wire-grid polarizer was incorporated in the instrument for measuring polarized spectra.

The normalized reflectance was calculated using a freshly aluminized front-surface mirror as a reference background. The plane of incidence was horizontal and the angle of incidence was approximately $7\frac{1}{2}°$. By orienting the sample so that the c axis in the face was either vertical or horizontal, either the π component ($E \| c$) or the σ component ($E \perp c$) of the polarized spectra could be individually excited.

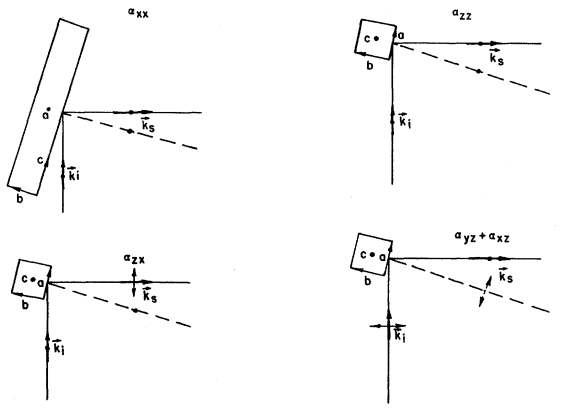

FIG. 1. Raman scattering geometries used for observing various Raman tensor components. The effective scattering geometry is approximately backward. The crystal axes are designated as a, b, and c. The polarization of the incident and the scattered light is referred to x, y, z axes fixed in space. The direction of light traveling inside the crystal projected backward is shown by the dashed line. The crystal a and b axes can be interchanged without changing the discussion in the text.

III. GROUP THEORY

Antimony sulphoiodide undergoes a ferroelectric first-order phase transition at about 288 °K. The crystal space group changes from D_{2h}^{16} ($Pnam$) to C_{2v}^{9} ($Pna2_1$) while the crystal class remains orthorhombic. At the second-order phase transition at about 233 °K, group-theoretical analysis shows that one of the following structural transitions can occur[11]:

$$C_{2v}^{9} \rightarrow C_s^1,\ C_s^2,\ C_2^2.$$

Measurements of pyroelectric anisotropy however indicate in favor of the transition[11]

$$C_{2v}^{9} \rightarrow C_2^2.$$

The full space-group symmetry has four formula units per unit cell.

In the interpretation of infrared transmission studies of SbSI powder, Blinc *et al.*[17] suggest the application of a simplified structure having only two SbSI units per unit cell and the symmetry change

$$C_{2h}^{2}\,(P2_{1/m}) \rightarrow C_2^2\,(P2_1).$$

The interaction between the adjacent double chains in SbSI structure can then be neglected and there are only two SbSI formula units in the unit cell. It

TABLE I. Number of optically active phonons in the proposed space groups of SbSI.

Lattice space group	Formula units	Number of optical modes	Optical activity: Infrared (electric dipole component)	Optical activity: Raman tensor components
		Full space group		
$(T>T_c)$ $D_{2h}^{16}(Pnam)$	4	33	2 B_{1u} $(E\parallel c)$ 5 B_{2u} $(E\parallel b)$ 5 B_{3u} $(E\parallel a)$	6 A_g $(\alpha_{xx}, \alpha_{yy}, \alpha_{zz})$ 6 B_{1g} (α_{xy}) 3 B_{2g} (α_{zx}) 3 B_{3g} (α_{yz})
$(T<T_c)$ $C_{2v}^{9}(Pna2_1)$	4	33	8 A_1 $(E\parallel c)$ 8 B_1 $(E\parallel a)$ 8 B_2 $(E\parallel b)$	(α_{xx}, yy, zz) 9 A_2 (α_{xy}) (α_{zx}) (α_{yz})
$T<T_c$ $C_2^2(P2_1)$	4	33	17 A $(E\parallel c)$ 16 B $(E\parallel a, E\parallel b)$	$(\alpha_{xx}, \alpha_{yy}, \alpha_{zz}, \alpha_{xy})$ $(\alpha_{zx}, \alpha_{yz})$
		Simplified space group		
$T>T_c$ $C_{2h}^{2}(P2_{1/m})$	2	15	2 A_u $(E\parallel c)$ 4 B_u $(E\perp c)$	6 A_g $(\alpha_{xx}, \alpha_{yy}, \alpha_{zz}, \alpha_{xy})$ 3 B_g $(\alpha_{xz}, \alpha_{yz})$
$T<Tc$ $C_2^2(P2_1)$	2	15	8 A $(E\parallel c)$ 7 B $(E\perp c)$	$(\alpha_{xx}, \alpha_{yy}, \alpha_{zz}, \alpha_{xy})$ $(\alpha_{xz}, \alpha_{yz})$

has been shown[2] that the room-temperature-phase Raman data are consistent with the simplified-space-group symmetry.

The number of Raman- and infrared-active modes for all full-space-group symmetries and simplified-space-group symmetries are summarized in Table I. The correlation diagrams between the irreducible representations of full-space-group symmetry change and simplified-space-group symmetry change are given in Fig. 2. The full-space-group symmetry in the paraelectric phase is D_{2h}^{16} $(Pnam)$. The factor group is isomorphic with the point-symmetry group D_{2h} of the crystal lattice. At the Γ point of the Brillouin zone, the Raman- or infrared-active optical phonons correspond to nonvanishing polarizability tensor or dipole moment components, respectively. Their number and symmetry is the same as irreducible representations of the point-symmetry group D_{2h} whose polarizability tensor components and dipole moment components are nonvanishing. According to group-theoretical analyses, the D_{2h} point group with 12 atoms per unit cell has 33 optical modes and 3 acoustic modes. Among the optical modes there are 18 Raman-active modes having the symmetries

$$6\,A_g + 6\,B_{1g} + 3\,B_{2g} + 3\,B_{3g}\,,$$

3 silent modes belonging to the A_u irreducible representation, and 12 infrared-active modes having $2\,B_{1u} + 5\,B_{2u} + 5\,B_{3u}$ irreducible representations.

In the ferroelectric phase after the first-order phase transition at 288 °K, the full-space-group symmetry changes to C_{2v}^{9}. We also find $6\,A_g + 2\,B_{1u} \rightarrow 8\,A_1$ modes, $3\,B_{2g} + 5\,B_{3u} \rightarrow 8\,B_1$ modes, and $3\,B_{3g} + 5\,B_{2u} \rightarrow 8\,B_2$ modes. These modes are both Raman and infrared active. We find the remaining modes $6\,B_{1g} + 3\,A_u \rightarrow 9\,A_2$ modes, which are only Raman active.

At the second-order phase transition at 233 °K the symmetry changes from $C_{2v}^{9} \rightarrow C_2^2$. Also, $8\,A_1 + 9\,A_2 \rightarrow 17\,A$ modes and $8\,B_1 + 8\,B_2 \rightarrow 16\,B$ modes, all simultaneously Raman and infrared active.

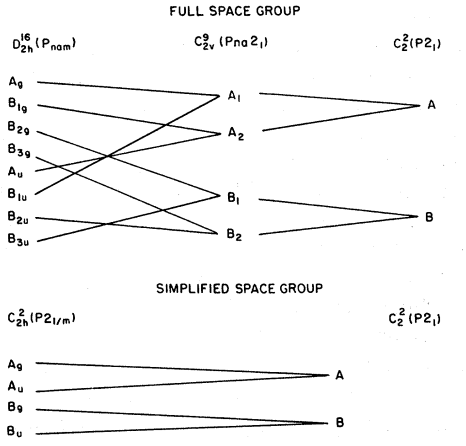

FIG. 2. Correlation diagrams of the symmetry change between the various space groups of SbSI.

In the simplified-space-group symmetry where the interaction between SbSI double chains is neglected, there are only two SbSI formula units in the unit cell. Since there are now six atoms per unit cell, there are 15 optical modes. In the paraelectric phase the symmetry is C_{2h}^2 and there are $6\,A_g + 3\,B_g$ Raman-active modes and $2\,A_u + 4\,B_u$ infrared-active modes. At the ferroelectric transition $C_{2h}^2 \rightarrow C_2^2$, $6A_g + 2A_u \rightarrow 8A$ modes and $4B_u + 3B_g \rightarrow 7B$ modes, and again all modes are both Raman and infrared active. The raman and infrared spectra in relation to these group-theoretical predictions are discussed below.

IV. RESULTS

A. Raman Spectra

According to group theory, (A_g, A) and (B_g, B) modes are allowed for α_{xx}, α_{yy}, α_{zz}, α_{xy}, and α_{yz}, α_{zx} polarizability tensor components, respectively. The corresponding Raman tensors are[18]

$$\alpha(A_g,A)=\begin{pmatrix} a & d & 0 \\ d & b & 0 \\ 0 & 0 & c \end{pmatrix}, \qquad \alpha(B_g,B)=\begin{pmatrix} 0 & 0 & e \\ 0 & 0 & f \\ e & f & 0 \end{pmatrix}.$$

The polarized Raman spectra were recorded at many temperatures down to 15 °K. In the paraelectric phase the spectra were shown in an earlier paper.[2] The results are summarized in Table II in which a new 239-cm^{-1} phonon has been included as reported recently.[4] Nine observed Raman-active modes of which six belong to A_g and three belong to B_g irreducible representation are in agree-

TABLE II. Assignments of Raman-active phonon modes (all frequencies are ±1 cm^{-1} of the values quoted), $T_c \simeq 288$ °K, $T' \simeq 233$ °K.

$T > T_c$ C_{2h}^2 (2 formula units) 299 °K		$T' < T < T_c$ C_2^2 (2 formula units) 250 °K	$T < T' < T_c$ C_2^2 (4 formula units)			
(cm^{-1})	Symmetry species	(cm^{-1})	100 °K (cm^{-1})	15 °K (cm^{-1})	Symmetry species	Raman tensor components
			41	41	A	α_{xx}, α_{zz}
			• • •	47	A	α_{zz}
		37[a], 29[b]	48[a], 30[b]	53[a], 33[b]	A	α_{zz}
51	A_g	54	58	• • •	A	α_{xx}
66	A_g	70	71	73	A	α_{xx}, α_{zz}
			• • •	92	A	α_{xx}
			96	98	A	α_{xx}
107	A_g	109	111	112	A	α_{xx}, α_{zz}
137	A_g	139	140	141	A	α_{xx}, α_{zz}
149	A_g	153	154	156	A	α_{xx}
		• • •	170	171	A	α_{zz}
		248	254	257	A	α_{xx}, α_{zz}
			258	262	A	α_{xx}
			314	317	A	α_{xx}
319	A_g	320	321	323	A	α_{xx}
37	B_g	39	• • •	43	B	α_{zx}
			54	55	B	α_{zx}
		59	60	63	B	α_{zx}
			68	70	B	α_{zx}
			78	79	B	α_{zx}
		119	121	123	B	α_{zx}
			125	126	B	α_{zx}
			• • •	136	B	α_{zx}
212	B_g	212	203	205	B	α_{zx}
			208	209	B	α_{zx}
239[c]	B_g	240	240	240	B	α_{zx}
			268	272	B	α_{zx}
			275	278	B	α_{zx}
			325	329	B	α_{zx}
		333	334	336	B	α_{zx}

[a]Strongly temperature-dependent mode.
[b]See Fig. 4. Weak band discussed in Ref. 3.
[c]See Ref. 4.

ment with theoretical predictions for the simplified-space-group symmetry due to Blinc *et al.* In the ferroelectric phase the spectra above 233 °K have been recorded at 250 °K. Six more new modes are now Raman active, namely, 29, 37, and 248 cm^{-1} of A symmetry and 54, 119, and 333 cm^{-1} of B symmetry. There are in all 8 A modes and 7 B modes observed in agreement with 15 theoretically allowed bands according to simplified-space-group symmetry C_2^2 having 2 SbSI formula units in a unit cell.

In the ferroelectric phase below 233 °K several bands begin to show additional structure. This results from a breakdown of the simplified-space-group-symmetry selection rules, and the full-space-group symmetry is now necessary for a complete interpretation of the low-temperature Raman spectra. The modes at 100 °K observed for all Raman polarizability tensor components are listed in Table II. The 320-cm^{-1} mode splits into three components at 314, 322 (A modes), and 325 cm^{-1} (B mode). The phonon at 248 cm^{-1} shifts and splits into 254- and 258-cm^{-1} A modes. The modes at

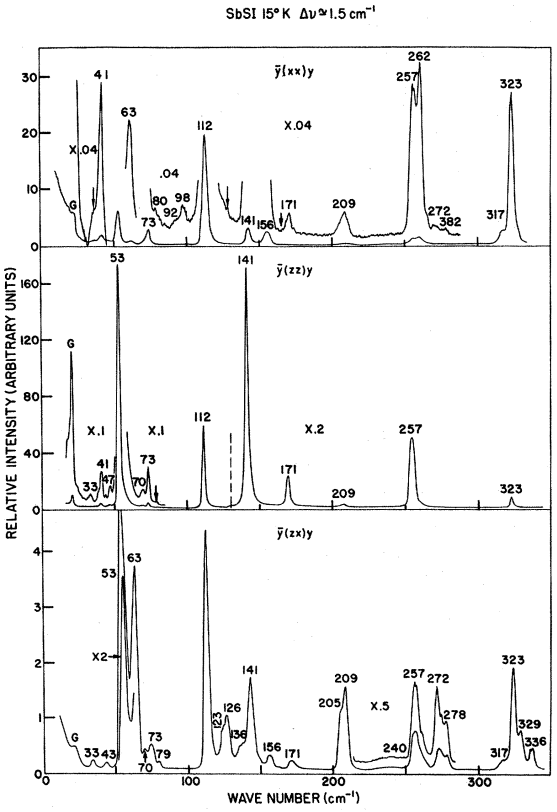

FIG. 3. Raman spectrum of SbSI at 15 °K. The bands labeled G are grating ghosts. The bands designated with an arrow (↓) are very weak bands, but may account for the missing phonon modes according to full space group C_2^2. $\Delta\nu$ is the spectral resolution of the instrument in wave numbers.

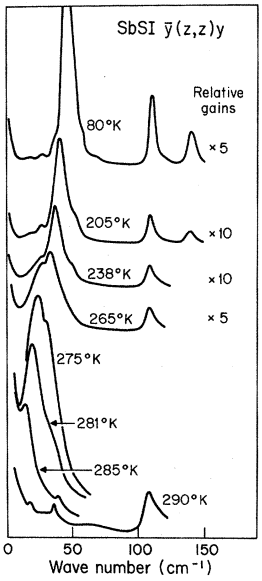

FIG. 4. Raman spectrum of SbSI measured for the α_{zz} polarizability tensor component in the soft-mode region, as a function of temperature. Relative gain factors have been used to indicate intensity changes with temperature.

121 and 125 cm^{-1} are just resolved from the strong 110-cm^{-1} mode. In all 14 A modes and 14 B modes were positively identified at 100 °K.

On further cooling down to 15 °K the splitting of most of the phonon modes is almost complete. Further splitting is observed of the 96-cm^{-1} mode which is now split into 92- and 96-cm^{-1} bands. The spectra observed at 15 °K is shown in Fig. 3. A total of 16 A modes and 14 B modes could be definitely identified at this temperature. This result is in close agreement with group-theoretical predictions for full-space-group symmetry C_2^2 ($P2_1$) of 17 A and 16 B modes. The missing 1 A modes and 2 B modes may be present in the spectra but they could not be identified with confidence.

The temperature-dependent Raman spectrum for $\bar{y}(zz)y$ in the ferroelectric phase is shown in Fig. 4. The level repulsion of two close A phonon states and the intensity transfer between the phonon modes of the same symmetry are also observed in our data.[3] The anticrossing frequency of the two phonons occurs between 265–275 °K which is in close agreement with the data of Harbeke *et al.*,[3] and these researchers suggest that the ferroelectric-paraelectric transition involves two coupled optical phonons of the same symmetry. However, our infrared data in the ferroelectric phase could not confirm such coupled-mode behavior possibly due to the second mode having only weak optical activity. In the paraelectric phase, symmetry considerations allow only two infrared-active modes for $c \parallel E$. The low-frequency soft mode at $\approx 9\ cm^{-1}$ and a strong mode around 179 cm^{-1} are the two positively identified allowed modes. The presence of a third mode of the same symmetry as the soft mode in the paraelectric phase should not be pres-

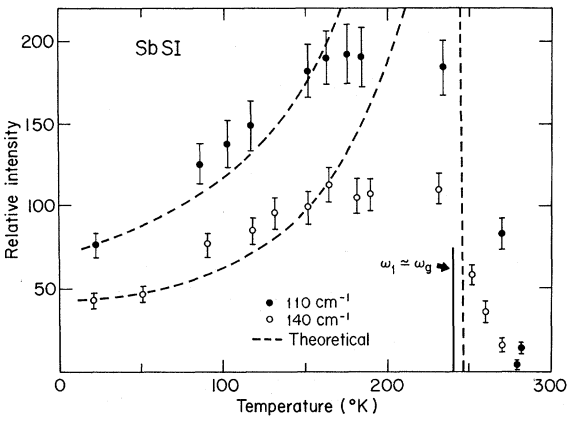

FIG. 5. Raman scattering intensities for 110- and 140-cm^{-1} bands plotted as a function of temperature. At about 240 °K the laser excitation energy coincides with the electronic band-gap energy ($\omega_1 \simeq \omega_g$).

ent by symmetry arguments and could not be observed.

The temperature dependence of the Raman frequencies and their widths was obtained over the entire temperature range. The Raman shifts for a high frequency (~319 cm^{-1}) and a lower frequency (~107 cm^{-1}) are ≈4 and ≈5 cm^{-1}, respectively. This result that Raman frequency shifts are lower for higher frequencies is in agreement with the theoretical conclusions involving third-order anharmonic forces given by Maradudin and Fein.[19] Similar conclusions were obtained by Vishwanathan from classical arguments.[20] The width of most of the lines (8–12 cm^{-1} at room temperature) decreased with decreasing temperature to 2 to 3 cm^{-1} at 15 °K. This agrees with the theoretical conclusion of Krishnan[20,21] that the half-widths should be approximately proportional to the square root of the absolute temperature.

B. Resonant Raman Effects

SbSI is a semiconductor material with room-temperature energy band gap of 1.88 eV for $E \| c$ and 1.95 eV for $E \perp c$.[22] The band gap shifts with temperature at an average rate $dE_g/dT \cong -1.5 \times 10^{-3}$ eV/°K.[23] The resonant enhancement of Rama scattering efficiency as the laser excitation energy approaches the band gap from below has been observed for several semiconductors.[24–26] Theoretically, the qualitative resonant Raman effects were explained by Loudon.[27,28]

In SbSI a marked increase of intensity is observed on cooling from T_c to 240 °K. Further cooling down to 15 °K results in a decreased intensity by a factor of about 3. The temperature dependence of the relative intensities of the 110- and 140-cm^{-1} bands have been measured using a $\bar{y}(zz)y$ configuration and the results are shown in Fig. 5. With the laser excitation energy 1.96 eV a rather broad maximum of the Raman scattering intensity is observed at ~ 200 °K for each phonon mode.

Using a two-band parabolic model,[28] the frequency dependence of the resonant term in the Raman tensor for direct-energy-gap semiconductors is found to be

$$R(-\omega_1, \omega_2, \omega_0) \propto \int_0^{K_{\max}} d\vec{K} \left[\left(\omega_g + \omega_0 - \omega_1 + \frac{K^2}{2\mu}\right)\left(\omega_g - \omega_1 + \frac{K^2}{2\mu}\right)\right]^{-1} \propto \left[(\omega_g + \omega_0 - \omega_1)^{1/2} - (\omega_g - \omega_1)^{1/2}\right], \quad (1)$$

where ω_1, ω_2, and ω_0 are the incident, Stokes, and lattice-vibration frequencies, respectively. The direct energy gap is $\hbar\omega_g$, the reduced mass is μ, and the electronic wave vector is $\vec{K}$. The Raman scattered intensity is proportional to the square of the Raman tensor $R(-\omega_1, \omega_2, \omega_0)$.

The Raman scattering intensities of the bands increase with increasing temperature due to resonant Raman effects as the band gap approaches the laser excitation energy from above. At about 240 °K the energy band gap $\hbar\omega_g$ coincides with the laser excitation energy. Raising the temperature further causes a sharp decrease in the Raman scattering efficiencies due to increased absorption in the crystal.

The theoretical intensity curves for the 110- and 140-cm^{-1} phonons according to Eq. (1) are also shown in Fig. 5. Comparison of the theoretical curves with the corresponding experimental data indicates a reasonably good agreement, when the band gap is more than about 5% above the laser excitation energy. In the temperature region around $\omega_1 \simeq \omega_g$, significant deviations of the experimental data from the theory are observed. A more refined theory in the vicinity of the energy gap, $\omega_1 \simeq \omega_g$, is necessary in order to take into account both the semiconducting and the ferroelectric effects.

C. Infrared Spectra

The infrared reflectivity spectra were obtained from the Fourier transform of the interferogram from a Michelson interferometer. Kramers-Kronig analysis of the reflectivity data gives the real and imaginary parts of the dielectric response function. The location of the TO modes is obtained as the peaks in $\omega\epsilon''$ and the longitudinal modes were located as peaks in $-\omega\eta''$, where $\eta = 1/\epsilon$, $\epsilon = \epsilon' + i\epsilon''$,

and $\eta'' = \mathrm{Im}(1/\epsilon)$.[29]

Polarized far-infrared reflectivity spectra have been measured in the wave-number region 20–400 cm^{-1}. The spectra for $c \| E$ have been measured at five fixed temperatures 298, 275, 210, 80, and 10 °K. For $c \perp E$, the spectra have been measured only at 298 and 80 °K, as no significant temperature variation of the modes were observed.

The spectra for $c \| E$ are shown in Figs. 6 and 7. At room temperature in the paraelectric phase, two bands are observed at ~9 and ~179 cm^{-1}.

The phonon mode at about 9 cm^{-1} is not Raman active in the paraelectric phase. In the far-infrared reflectivity spectra Petzelt[1] reported a band at ~22 cm^{-1} at 25 °C. However, the reported reflectivities in the low-frequency region are probably low by 15 to 20% of the correct values due to the porosity and the fibrous nature of the material. Recently Sugawara and Nakamura[5] reported far-infrared reflectivities for $E \| c$ at 300 and 83 °K. Their low-frequency reflectivities, when properly scaled to account for surface imperfections of the crystal (about 5%), agreed with those calculated from static dielectric constant values. A Kramers-Kronig analysis of their 300 °K data then yielded a very-low-frequency soft mode around a few wave numbers. Our low-frequency room-temperature experimental data and subsequent Kramers-Kronig analysis is in close agreement with the results of Sugawara and Nakamura. Scaling of Petzelt's measurements so that the extrapolated value of the reflectivity at zero frequency agrees with that calculated from static dielectric constant data lowered the 22-cm^{-1} band to the vicinity of 5–15 cm^{-1}. Consequently Petzelt's conclusion that the 22-cm^{-1} mode accounted for only about 10% of the static dielectric constant is probably incorrect and his rather low absolute values of the reflectance may be due to sample porosity.

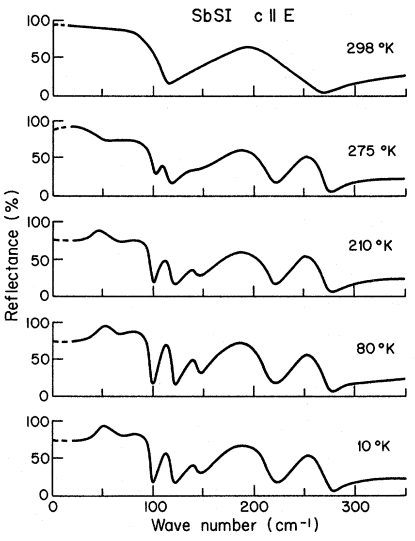

FIG. 6. Far-infrared reflectivity spectra of SbSI for $c \| \vec{E}$ at 298, 275, 210, 80, and 10 °K. The spectra at 275 and 10 °K beyond 250 cm^{-1} and below 20 cm^{-1} have been extrapolated in order to perform the Kramers-Kronig analysis.

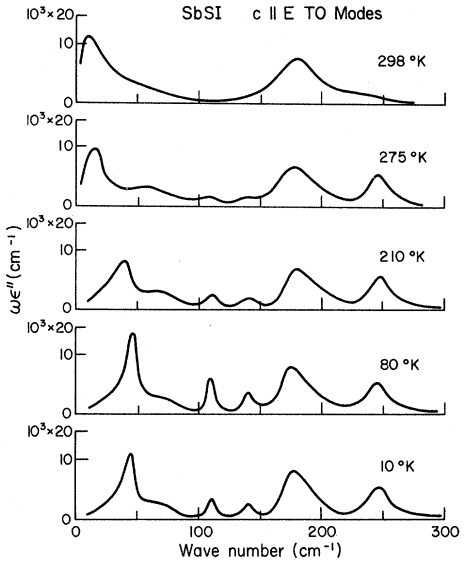

FIG. 7. TO phonons for $c \| E$ at the Brillouin-zone center ($k \sim 0$) obtained by Kramers-Kronig analysis of the reflectivity data derived as peaks in $\omega\epsilon''$.

The dielectric dispersion obtained from our reflection data by a Kramers-Kronig analysis gives the location of TO- and LO-phonon frequencies. The TO-phonon modes are shown in Fig. 7. For the TO mode at ~9 cm^{-1} the corresponding LO mode is at ~111 cm^{-1}. Disregarding the contribution of all the other modes to the static dielectric constant, the Lyddane-Sachs-Teller relation for a single infrared-active mode is

$$\epsilon_0/\epsilon_\infty = \omega_L^2/\omega_T^2 \ , \qquad (2)$$

where ω_T and ω_L are the TO- and LO-mode frequencies and ϵ_0 and ϵ_∞ are the static and high frequency dielectric constants, respectively, parallel to the c axis. Taking $\epsilon_\infty = n_\infty^2 \simeq 25$, $\omega_L \simeq 111$ cm^{-1}, and $\omega_T \simeq 9$ cm^{-1}, Eq. (2) gives for $\epsilon_0 \simeq 3800$, indicating that this mode, in fact, contributes more than 90% to the room-temperature observed value ~4500.[30]

The fact that the mode at ~9 cm^{-1} is the 22-cm^{-1} mode reported by Petzelt and not a new mode is further supported by group-theoretical predictions; that for both the full-space-group symmetry and the simplified-space-group symmetry in the paraelectric phase for $c \| E$ only two modes are infrared active. The modes have been found at ~9

TABLE III. Transverse and longitudinal $k \approx 0$ infrared-active phonons[a] (all modes are ± 5 cm^{-1} of the values quoted unless otherwise noted) in the paraelectric and ferroelectric phases of SbSI for $E \| c$.

	$T > T_c$ (C_{2h}^2) (2 formula units) 298 °K		$T < T_c$ (C_2^2) (2 formula units) 275 °K	210 °K	80 °K	10 °K
ω_T	9	ω_T	16	42	46	45
		ω_L[b]	...	...	...	...
		ω_T	60	66	68	68
ω_L	111	ω_L	100	98	98	98
		ω_T	108	110	110	110
		ω_L	115	118	119	119
		ω_T	138	140	140	140
		ω_L	140	142	143	143
ω_T	179 ± 10	ω_T	178 ± 10	180 ± 10	175 ± 10	176 ± 10
		ω_L	217 ± 10	217 ± 10	217 ± 10	217 ± 10
		ω_T	247	247	247	247
ω_L	261 ± 10	ω_L	271	271	271	271

[a]All modes are ± 5 cm^{-1} of the values quoted unless otherwise noted.
[b]Not observed.

and 179 cm^{-1}.

The location of all the TO and LO modes for $c \| E$ in both the paraelectric and the ferroelectric phases are summarized in Table III. In the ferroelectric phase there are six observed modes. According to the simplified symmetry, group theory predicts eight modes. Thus the observed data is consistent with the simplified space group C_2^2 ($P2_1$). The Raman data indicate that the full space group is more appropriate to interpret the optical modes in the ferroelectric phase. However, the infrared modes are rather broad especially the bands around 50, 66, and 176 cm^{-1}. Consequently the weak phonon modes allowed by the full-space-group symmetry cannot be resolved even at low temperatures and are completely masked by the stronger bands.

The infrared spectra for $c \perp E$ have been measured at 298 and 80 °K. The spectra are shown in Fig. 8 and the results are summarized in Table IV. In the paraelectric phase, four bands at 78, 120, 270, and 327 cm^{-1} are identified as B_u modes in agreement with the simplified symmetry theoretical predictions. The bands at 56 and 66 cm^{-1} reported by Petzelt[1] are not observed in our data. Possibly these two bands could be the A_g Raman-active modes at 51 and 66 cm^{-1} made infrared active due to strain in the material. Similar effects are indicated in the transmission data of powders reported by Blinc *et al.* in which several strong A_g Raman-active modes were observed in the infrared spectrum in the paraelectric phase. In the ferroelectric phase, six bands at 80, 124, 245, 270, 320, and 332 cm^{-1} are observed. This is close to seven B modes predicted by group theory with the simplified unit cell assumption.

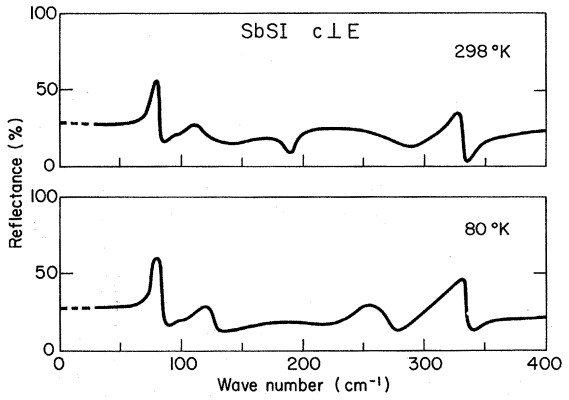

FIG. 8. Far-infrared reflectivity spectra of SbSI for $c \perp \vec{E}$ at 298 and 80 °K. The spectra below 50 cm^{-1} have been extrapolated to 0 cm^{-1}.

D. Soft-Mode Behavior

In the ferroelectric phase in the submillimeter wave region a TO band shifting from 16 cm^{-1} at 275 °K to 46 cm^{-1} at 80 °K accounts completely for the temperature dependence of the static dielectric constant. A similar shift with temperature is observed in the Raman data. Temperature dependence of ω_{TO} observed from both the infrared and the Raman data is shown in Fig. 9. On the same plot $(A) \times 10^3/[\epsilon_0(T)]$, $^{1/2}$ where $\epsilon_0(T)$ are taken from Ref. 30, is also shown. It is seen that within the experimental error there is good agreement between the infrared and the Raman data and the temperature dependence of the dielectric constant.

Application of Cochran's theory for displacive ferroelectrics[13] to noncubic crystals can be made using the generalized Lyddane-Sachs-Teller relationship

TABLE IV. Transverse and longitudinal $k \approx 0$ infrared-active phonons (all modes are ± 5 cm^{-1} of the values quoted, unless otherwise indicated) in the paraelectric and ferroelectric phases of SbSI for $E \| c$.

$T > T_c$ (C_{2h}^2) (2 formula units) 298 °K		$T < T_c$ (C_2^2) (2 formula units) 80 °K	
ω_T	78	ω_T	80
ω_L	82	ω_L	85
ω_T	120	ω_T	124
ω_L	124	ω_L	128
		ω_T	245 ± 10
		ω_L	250 ± 10
ω_T	270	ω_T	270
ω_L	276	ω_L	272
		ω_T	~320
		ω_L[a]	...
ω_T	327	ω_T	332
ω_L	332	ω_L	334

[a]Not observed.

$$\frac{\epsilon_0(l)}{\epsilon_\infty(l)} = \prod_i \frac{\omega_{L_i}(l)^2}{\omega_{T_i}(l)^2} \quad ,$$

where l refers to the l axis of the crystal.

The logarithmic differential form of this equation has been derived by Barker[31] and allows measurements of the contributions of phonons to the dielectric constant below T_c:

$$\frac{\Delta\epsilon_0}{\epsilon_0} = \frac{2\Delta\omega_{L_1}}{\omega_{L_1}} + \frac{2\Delta\omega_{L_2}}{\omega_{L_2}} + \cdots - \frac{2\Delta\omega_{T_1}}{\omega_{T_1}} - \frac{2\Delta\omega_{T_2}}{\omega_{T_2}} - \cdots .$$

If only ω_{T_1} is significantly temperature dependent then

$$\frac{\Delta\epsilon_0}{\epsilon_0} \simeq -\frac{2\Delta\omega_{T_1}}{\omega_{T_1}} .$$

These two quantities are in reasonably good agreement as shown previously in Ref. 2. In Fig. 9 the close agreement of the infrared and the Raman data and the dielectric-constant data also confirms the hypothesis that SbSI is a displacive ferroelectric similar to the perovskites.

V. CONCLUSIONS

Polarized infrared and Raman spectra of SbSI have been measured in both the paraelectric and ferroelectric phases as a function of temperature. The frequencies and the symmetries of most of the optical phonons have been determined in both phases. It has been found that full-space-group symmetry C_2^2 (4 formula units/unit cell) is required in the complete interpretation of the low-temperature (< 233 °K) Raman data. The simplified space group proposed by Blinc *et al.* is applicable to the major features of Raman and infrared spectra at room temperature but breaks down at low temperatures in the ferroelectric phase. This is due to the fact that many of the sharp but weak Raman modes observed at low temperatures are rapidly damped out at higher temperature due to lattice anharmonicity.

The soft-mode behavior for the first-order phase transition at 288 °K has been observed in both the paraelectric and the ferroelectric phases. In the paraelectric phase, the low-frequency mode is situated at less than 10 cm^{-1} at room temperature and accounts for more than 90% of the quoted values of the static dielectric constant. In the ferroelectric phase, the soft-mode behavior has been observed in both the Raman and the infrared spectra. Its temperature dependence is in agreement with the temperature dependence of dielectric constant $\epsilon_0(T)$ as $\omega_{T_0} \propto 1/[\epsilon_0(T)]^{1/2}$, confirming the displacive nature of the phase transition in SbSI. The soft mode in the ferroelectric phase passed smoothly through the second-order phase transition $C_{2v}^9 \rightarrow C_2^2$ at 233 °K. Our temperature-dependent Raman data in the ferroelectric phase are in close agreement with the results of Harbeke *et al.* However their coupled-mode-behavior observation could not be confirmed in our infrared measurements in the ferroelectric or the paraelectric phases. No doubt the infrared activity of this mode is extremely weak and its presence could not be distinguished from the dominant soft mode in either phase. Also group theoretically, the presence of another lower-frequency mode is excluded in the paraelectric phase. Resonant enhancement of Raman scattering efficiency has been observed at about 240 °K where the electronic band-gap energy coincides with the

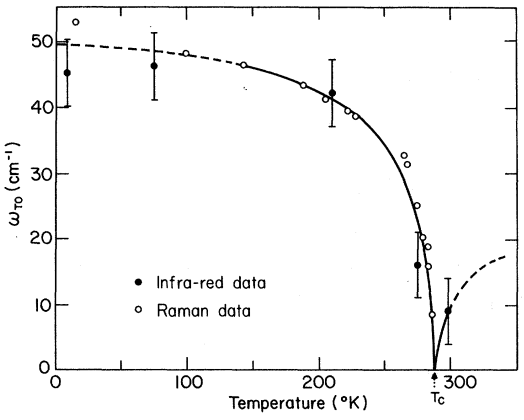

FIG. 9. Temperature dependence of the ferroelectric mode frequency. The solid line is a plot of $(A \times 10^3)/[\epsilon_0(T)]^{1/2}$. The dielectric-constant data have been taken from Ref. 30. A has been found to be 26.3 in the ferroelectric phase and 23.2 in the paraelectric phase.

laser excitation energy of 1.96 eV.

ACKNOWLEDGMENTS

The authors would like to thank Dr. B. Molnar, Physical Electronics Department, Ford Motor Co., Dearborn, Mich., and Dr. G. Taylor, R.C.A., Princeton, N. J., for the samples. This work forms a part of the thesis of one of us (D.K.A.) to be submitted to Northeastern University, Physics Department, in partial fulfillment of the requirements for the Ph.D. degree.

---

†Work supported in part by a Northeastern Grant for Basic Research and by NASA under Grant No. NGL 22-011-051.

[1]J. Petzelt, Phys. Status Solidi 36, 321 (1969).

[2]C. H. Perry and D. K. Agrawal, Solid State Commun. 8, 225 (1970).

[3]G. Harbeke, E. F. Steigmeier, and R. K. Wehner, Solid State Commun. 8, 1765 (1970).

[4]M. Balkanski, M. K. Teng, S. M. Shapiro, and M. K. Ziolkiewicz, Phys. Status Solidi (to be published).

[5]F. Sugawara and T. Nakamura, in *Proceedings of the Second International Meeting on Ferroelectricity, Physics Society of Japan*, 1970 (Science Council of Japan, Kyoto, 1970), pp. 221, 222.

[6]E. Fatuzzo, G. Harbeke, W. J. Merz, R. Nitsche, H. Roetschi, and W. Ruppel, Phys. Rev. 127, 2036 (1962).

[7]T. Mori, H. Tamura, and E. Sawaguchi, J. Phys. Soc. Japan 20, 1294 (1965).

[8]B. Molnar, R. Johannes, and W. Haas, Bull. Am. Phys. Soc. 10, 109 (1965).

[9]A. Kikuchi, Y. Oka, and E. Sawaguchi, J. Phys. Soc. Japan 23, 337 (1967).

[10]T. Takama and T. Mitsui, J. Phys. Soc. Japan 23, 331 (1967).

[11]D. M. Bercha, I. V. Bercha, V. Y. Slivka, I. D. Turyanitsa, and D. V. Chepur, Fiz. Tverd. Tela 11, 1677 (1969) [Sov. Phys. Solid State 11, 1356 (1969)].

[12]V. N. Nosov, Kristallografiya 13, 338, (1968) [Sov. Phys. Crist. 13, 273 (1968)].

[13]W. Cochran, Advan. Phys. 9, 387 (1960).

[14]N. E. Tornberg and C. H. Perry, Appl. Opt. 9, 777 (1970).

[15]R. Johannes and W. Haas, Appl. Opt. 6, 1059 (1967).

[16]C. H. Perry, R. Geick, and E. F. Young, Appl. Opt. 5, 1171 (1966).

[17]R. Blinc, M. Mali, and A. Novak, Solid State Commun. 6, 327 (1968).

[18]R. Loudon, Advan. Phys. 13, 423 (1964).

[19]A. A. Maradudin and A. E. Fein, Phys. Rev. 128, 2589 (1962).

[20]K. S. Vishwanathan, Can. J. Phys. 41, 423 (1963).

[21]R. S. Krishnan, Proc. Indian Acad. Sci. A24, 45 (1946).

[22]G. Harbeke, J. Phys. Chem. Solids 24, 957 (1963).

[23]R. Kern, J. Phys. Chem. Solids 23, 243 (1962).

[24]R. C. C. Leite, T. C. Damen, and J. F. Scott, in *International Conference on Light Scattering Spectra of Solids*, 1968, edited by G. B. Wright (Springer, New York, 1969), p. 359.

[25]R. K. Chang, J. M. Ralston, and D. E. Keating, in Ref. 24, p. 369.

[26]E. M. Anastassakis and C. H. Perry, Solid State Commun. 9, 407 (1971).

[27]R. Loudon, J. Phys. (Paris) 26, 677 (1965).

[28]R. Loudon, Proc. Roy. Soc. (London) A275, 218 (1963).

[29]R. P. Lowndes, J. F. Parrish, and C. H. Perry, Phys. Rev. 182, 913 (1969).

[30]Y. Masuda, K. Sakata, S. Hasegawa, G. Ohara, M. Wada, and M. Nishizawa, Japan J. Appl. Phys. 8, 692 (1969).

[31]A. S. Barker, Jr., in *Ferroelectricity*, edited by E. F. Weller (Elsevier, Amsterdam, 1967), p. 238.